ISIJ International, Vol. 41 (2001), Supplement, pp. S73-S80

— *Review* —

Creep Deformation Behaviour and Kinetic Aspects of 9Cr-1Mo Ferritic Steel

B. K. Choudhary, C. Phaniraj, K. Bhanu Sankara Rao and S. L. Mannan

Mechanical Metallurgy Division, Indira Gandhi Centre for Atomic Research, Kalpakkam - 603 102, India

This paper presents the detailed investigations on creep behaviour of 9Cr-1Mo ferritic steel with an emphasis to understand and unify the different stages of creep deformation in the framework of first order kinetic approach. The different values of stress exponent and apparent activation energy observed for the two stress regimes have been rationalized by invoking the concept of resisting stress. The detailed analysis of results revealed that both transient and tertiary creep obeyed first order kinetics with separate values of transient and tertiary creep parameters in the respective stress regimes. The two stress regimes with different values of stress exponent are manifested as separate master creep curves for transient and steady state creep. Similarly, the analysis of tertiary creep also revealed distinct master creep curves relating steady state and tertiary creep in the respective stress regimes. The paper also focuses attention on two important relationships, one obtained between transient and steady state creep, and the other between steady state and tertiary creep. The useful implications of these relationships in understanding the existing creep rate-rupture life relationships of Monkman-Grant type are also highlighted in this paper.

KEY WORDS: 9Cr-1Mo ferritic steel; steady state creep; first order kinetics; transient creep; tertiary creep; Monkman-Grant relation.

1. Introduction

The advent of new generation power plants have increased the operating steam temperatures and pressures to achieve higher efficiency and better environmental protection. This has led to the development of 9Cr-1Mo steel and its modified versions with excellent combination of creep strength and ductility for steam generator applications. The modified versions mainly include 9Cr-1Mo steel initially modified by the addition of strong carbide forming elements such Nb and V, and further modified by the addition of W, i.e. 9Cr-0.5Mo-1.8W; these have been designated as P91 and P92 respectively according to ASTM standards. Reduced Mo and W added P92 steel is the same as Japanese NF616 steel. As already mentioned, the driving force in the development of these advanced 9Cr-1Mo steels is to achieve improved creep properties, it is therefore essential to emphasize that understanding of creep behaviour is of paramount importance.

Steady state creep behaviour of low alloy ferritic steels[1,2] and 9Cr-1Mo steel[3,4] have shown two stress regimes with different values of stress exponent and apparent activation energy. A similar two exponent behaviour has also been observed recently for a P92 steel.[5] However, the rationalization of these observed deviations in terms of effective stress has not been attempted in the past for 9Cr-1Mo steel and its modified versions. The systematic investigations addressing the various aspects of creep behaviour of 9Cr-1Mo steel are presented in this paper. The purpose of this paper is mainly two fold; the first is to rationalize the two stress regimes by invoking the concept of resisting stress and the second is to unify the different stages of creep deformation in the framework of first order kinetics. The paper also focuses attention on important relationships obtained for transient and tertiary creep obeying first order kinetics[6-9] and their implications in understanding the existing creep rate-rupture life relationships of Monkman-Grant type.[10,11] The rationalization of steady state creep behaviour in terms of resisting stress is dealt in the following section.

2. Steady State Creep Behaviour

The dependence of steady state creep rate $\dot{\epsilon}_s$ on applied stress σ_a and temperature at high temperatures for pure metals and solid solution alloys is well described by the Dorn's relationship[12]

$$\dot{\epsilon}_s = ADμb/(kT)\ (\sigma_a/\mu)^n, \qquad (1)$$

with $D = D_0 \exp(-Q/RT)$, where D is the lattice self diffusion coefficient, D_0 is the frequency factor, Q is the activation energy, R is the gas constant, μ is the shear modulus, b is the Burgers vector, k is Boltzmann's constant, n is the stress exponent and A is a dimensionless constant. Further, the observed value of n between 4 and 5 and activation energy nearly equal to that for self diffusion

process are well interpreted by Eq. (1) and are in agreement with that predicted by recovery creep theories. On the contrary, the applicability of Eq. (1) for particle and precipitation strengthened alloys gives rise to unrealistically high values of stress exponent and apparent activation energy.[1-5,13,14] These difficulties have been overcome by rationalizing in terms of effective stress as

$$\dot{\epsilon}_s = A_0 D\mu b/(kT) \quad [(\sigma_a - \sigma_R)/\mu]^{n_o}, \qquad (2)$$

where σ_R is the threshold or resisting stress associated with the operative particle-by-pass mechanism, n_0 is the modified stress exponent equal to about 4 and A_0 is a dimensionless constant.

Before presenting the detailed analysis of creep, it is necessary that we describe briefly the experimental details. 9Cr-1Mo steel forging (1000 mm diameter and 300 mm thickness) was supplied in quenched and tempered condition (Q+T: 1223 K/5 h, water quenched and 1023 K/8 h, air cooled). The additional heat treatments viz. simulated post-weld heat treatment (SPWHT: 998 K/3 h, with heating and cooling rates of 50 K h^{-1} above 673 K) and thermally aged (TA: 793 K /5000 h) conditions were also employed for creep testing. The results of constant load creep tests conducted at temperatures ranging from 773 to 873 K and at stresses ranging from 50 to 300 MPa are used for the detailed analysis of creep behaviour of this steel. The details regarding material, microstructures and creep testing are described elsewhere[15-17].

2.1. Stress and temperature dependence of steady state creep rate

For different heat treatment conditions and at all test temperatures, the dependence of $\dot{\epsilon}_s$ on σ_a obeyed power-law relation as shown in **Fig. 1** and further revealed two slope behaviour with different values of stress exponent n = 5.5 and 10.2 for low and high stress regimes, respectively. The differences in creep rates for different heat treatment conditions have been described elsewhere.[15] In the high stress regime, the apparent activation energy Q_{app} = 468 ± 10 kJ mol^{-1} was determined from plots of $\log\dot{\epsilon}_s$ vs 1/T. Whereas at low stresses, Q_{app} = 268 kJ mol^{-1} was obtained from temperature jump tests. The two stress regimes characterized by different values of stress exponent and activation energy are in accordance with those reported for 9Cr-1Mo steel[3,4], P92 steel[5] and for other precipitation hardened alloys.[13,14] However, the apparent activation energy values observed in this study need to be corrected for variation of shear modulus with temperature. It follows from Eq. (1) that the modulus compensated activation energy can be obtained from a semi-logarithmic plot of $\dot{\epsilon}_s\,\mu^{n-1}$ T against 1/T and for high stress regime (with n = 10.2) Q is obtained as 418 ± 13 kJ mol^{-1}. At low stresses, the modulus compensated activation energy is obtained as 255 kJ mol^{-1}. Unlike in the low stress regime, the Q value of 418 ± 13 kJ mol^{-1} obtained in the high stress regime even after modulus correction is significantly higher than that for self diffusion in

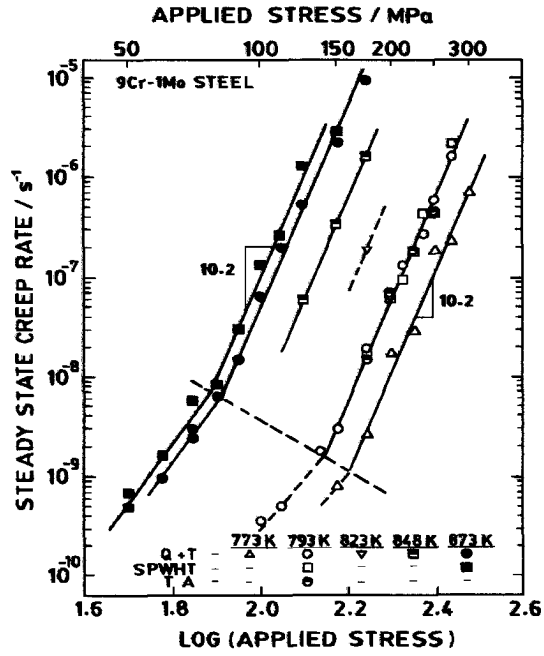

Fig. 1 Stress dependence of steady state creep rate for 9Cr-1Mo steel

α-iron, i.e. Q_{SD} = 250 kJ mol^{-1} and this prompted us to rationalize the steady state creep behaviour by invoking the concept of resisting stress.

2.2. Resisting stress and rationalization of steady state creep

It is already mentioned that Eq. (2) can be successfully used to interpret the steady state creep behaviour of particle and precipitation strengthened alloys in terms of effective stress, which is the difference between the applied stress and the resisting stress. Based on the experimental observations, it is now well accepted that in the low stress regime (with n ~ 4), σ_R linearly increases with σ_a (i.e. $\sigma_R = K.\sigma_a$) and approaches a constant threshold stress σ_H in the high stress regime (with n significantly higher than 4) at $\sigma_a > \sigma_T$; σ_T is the transition stress. σ_R values reported in this study are determined from the creep data using the graphical method proposed by Lagneborg and Bergman[13], which assumes that the mechanism changes from climb by-pass over particles to Orowan bowing or particle shearing at $\sigma_a > \sigma_T$. Equation (2) indicates that a linear plot $(\dot{\epsilon}_s)^{1/n_o}$ vs σ_a yields two straight lines one for low and other for high stress regime, and σ_H is obtained as the stress intercept by extrapolating the second straight line (i.e. pertaining to high stress regime) to $\dot{\epsilon}_s = 0$. At low stresses, σ_R is obtained from $\sigma_R = K.\sigma_a$, where K is evaluated as the ratio of σ_H/σ_T.

Our attempt to determine σ_R for different test conditions is shown in **Fig. 2**, where $(\dot{\epsilon}_s\, kT/D\mu b)^{1/4}$ is plotted against σ_a/μ, and the values of D, μ and b for α-iron are taken from Ref. (18). The value of n_0 = 4 chosen in **Fig. 2** is in order because it yielded best fit parallel lines at high stresses and further is in accordance with the theory proposed by Lagneborg and Bergman.[13] It is interesting to note that at low stresses, the diffusivity term

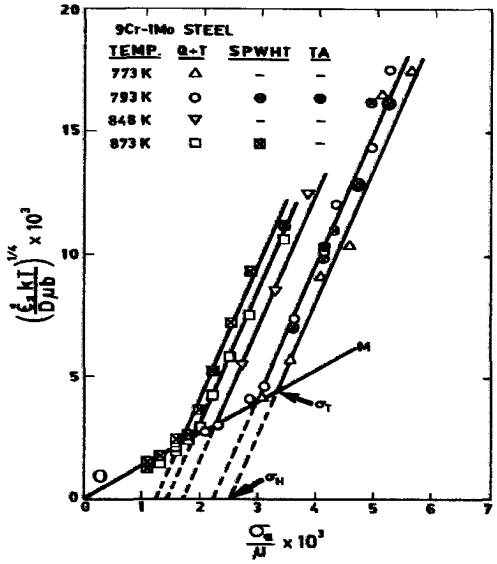

Fig. 2 $(\dot{\epsilon}_s kT/D\mu b)^{1/4}$ vs σ_a/μ plot for 9Cr-1Mo steel

is able to absorb the differences in creep rates and bring together the data onto a single line (i.e. OM in **Fig. 2**). This suggests that creep is governed by climb by-pass mechanism at low stresses. The σ_H values are determined from **Fig. 2** as the stress intercepts at $\dot{\epsilon}_s = 0$ and intersection of parallel lines with OM gives σ_T values. Another important result is that for different test conditions at low stresses, σ_R is proportional to σ_a with proportionality constant K = 0.77 and is in agreement with that predicted by Lagneborg and Bergman[13] and the reported values in the lietrature.[1,2] Higher value of n = 5.5 (than assumed value of 4) observed at low stresses could be related to internal stress due to dislocation substructure and/or absolute threshold stress. The rationalization of $\dot{\epsilon}_s$ in terms of effective stress at various temperatures is typically shown in **Fig. 3** for Q + T condition revealing a single slope behaviour for both the stress regimes.

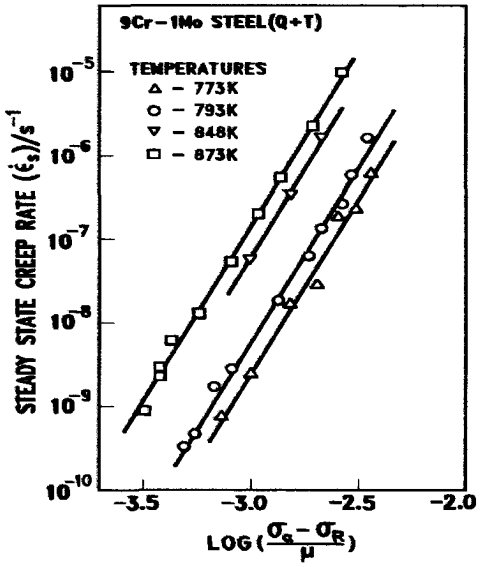

Fig. 3 $\dot{\epsilon}_s$ vs $(\sigma_a - \sigma_R)/\mu$ plot for 9Cr-1Mo steel in Q + T condition

Following Eq. (2) and at a constant $(\sigma_a-\sigma_R)/\mu$ value of 1 x 10^{-3}, plot of $\dot{\epsilon}_s \mu^{-1}$ T vs 1/T is shown in **Fig. 4** and the true activation energy is determined as 237 kJ mol^{-1}, which is close to Q_{SD} = 250 kJ mol^{-1} for α-iron. The rationalization of steady state creep behaviour in both the stress regimes for different test conditions with a single stress exponent value of ~ 4 is shown in **Fig. 5**. From the analysis presented so far, we conclude that the steady state creep deformation is controlled by dislocation climb process in both the stress regimes. In order to obtain further understanding of the manifestations observed in the two stress regimes, the detailed analysis of creep is carried out in the framework of first order kinetics[19] and is described in the following section.

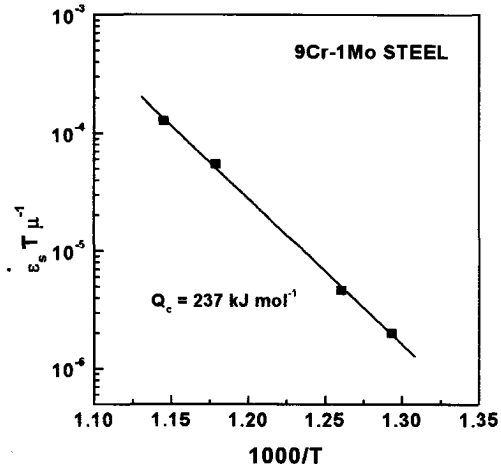

Fig. 4 $\dot{\epsilon}_s T \mu^{-1}$ vs 1000/T plot for Q + T condition at constant $(\sigma_a - \sigma_R)/\mu = 1 \times 10^{-3}$

3. First Order Kinetics for Creep

The first order kinetic approach is based on the premise that the rearrangement of dislocations at all stages of creep deformation is governed by climb controlled first order rate process. The unified description of transient and

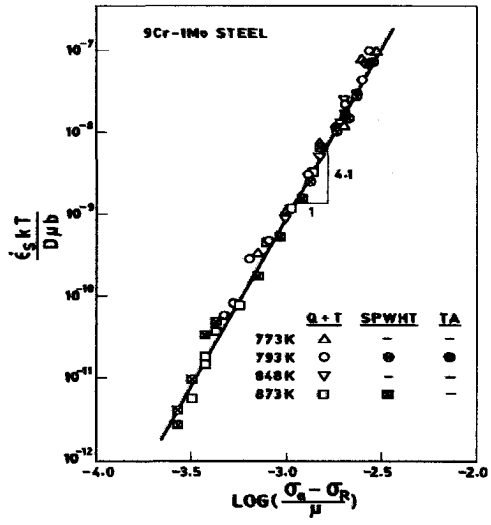

Fig. 5 $(\dot{\epsilon}_s kT/D\mu b)$ vs $(\sigma_a - \sigma_R)/\mu$ plot for 9Cr-1Mo steel

tertiary creep and the useful implications of kinetic approach to understand the creep rate-rupture life relationships mainly form the contents of this section.

3.1. Transient creep

The transient and steady state creep as a first order process proposed by Webster, Cox and Dorn[20] and subsequently developed by Dorn, Mukherjee and coworkers[21,22] is couched in terms of creep rate $\dot{\epsilon}$ as $d(\dot{\epsilon} - \dot{\epsilon}_s)/dt = -(\dot{\epsilon} - \dot{\epsilon}_s)/\tau$, where τ is the relaxation time for rearrangement of dislocations and $1/\tau$ is the rate constant which depends on stress and temperature in same way as does $\dot{\epsilon}_s$ ($1/\tau = K.\dot{\epsilon}_s$, K = constant). Integrating twice the above formulation leads to the well known Garofalo[23] strain-time relation

$$\epsilon = \epsilon_0 + \epsilon_T [1 - \exp(-r.t)] + \dot{\epsilon}_s.t, \qquad (3)$$

where ϵ_0 is the initial strain at time t = 0, ϵ_T is the limiting transient creep strain and r is the rate of exhaustion of transient creep and is the same as rate constant $1/\tau$ when transient creep obeys first order kinetics. Another important prediction is the proportionality between the initial creep rate $\dot{\epsilon}_i$ and $\dot{\epsilon}_s$, i.e. $\dot{\epsilon}_i = \beta.\dot{\epsilon}_s$, where β is a constant > 1. The important outcome of this approach is the universal creep equation of the form

$$\epsilon - \epsilon_0 = (\beta - 1)/K [1 - \exp(-K.\dot{\epsilon}_s.t)] + \dot{\epsilon}_s.t, \qquad (4)$$

where $(\beta - 1)/K = \epsilon_T$. It is emphasized that ϵ_T is a constant, since β and K are constants. Further for a constant ϵ_T, Eq. (4) yields a single master creep curve when the data is plotted as $(\epsilon - \epsilon_0)$ vs $\dot{\epsilon}_s.t$. Strain-time data obtained for 9Cr-1Mo steel at different test conditions obeyed Eq. (3), and ϵ_0 and ϵ_T were determined from the normal creep curves. r was evaluated graphically as the slope of $\ln(1 - \Delta/\epsilon_T)$ vs t plots, where Δ is the transient creep component ($\Delta = \epsilon - \epsilon_0 - \dot{\epsilon}_s.t$); $\Delta = 0$ at t = 0 and approaches ϵ_T at $t = t_{os}$, i.e. the time for the onset of steady state creep. Following Eq. (3), $\dot{\epsilon}_i$ was calculated as $\dot{\epsilon}_i = \dot{\epsilon}_s + r\epsilon_T$.

Contrary to pure metals and austenitic stainless steels,[6,21,22] the high stress results for 9Cr-1Mo steel could not be described by a single master creep curve (e.g., at 873 K for Q + T condition in **Fig. 6**) according to Eq. (4), since ϵ_T increased with decreasing stress. Further, the proportionality between r and $\dot{\epsilon}_s$ ($r = K.\dot{\epsilon}_s$) is not observed in the high stress regime (e.g., at 793 K for Q + T condition in **Fig. 7**). Whereas at low stresses, for a particular temperature, K is found to be constant (**Fig. 7**) and the constancy of ϵ_T resulted in a single master curve. While $\dot{\epsilon}_i$ is proportional to $\dot{\epsilon}_s$ ($\dot{\epsilon}_i = \beta.\dot{\epsilon}_s$) for all test conditions as seen in **Fig. 8**, the proportionality constant β is different at low stresses ($\beta = 15$) and at high stresses ($\beta = 4.1$). It is already seen in **Fig. 6** that Eq. (4) failed to provide the unified master creep curve, since ϵ_T and K

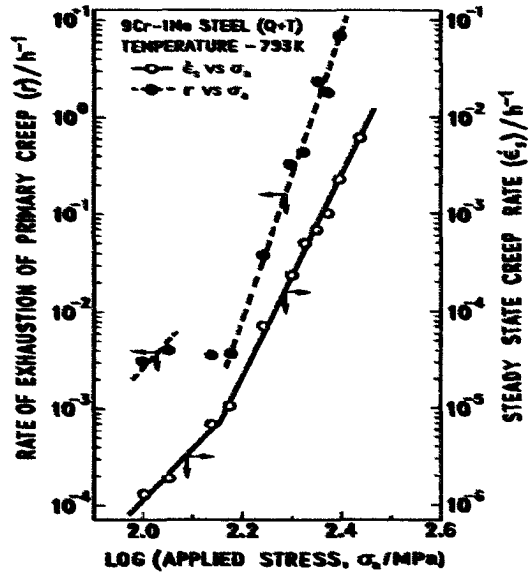

Fig. 7 Stress dependence of r and $\dot{\epsilon}_s$ for results at 793 K

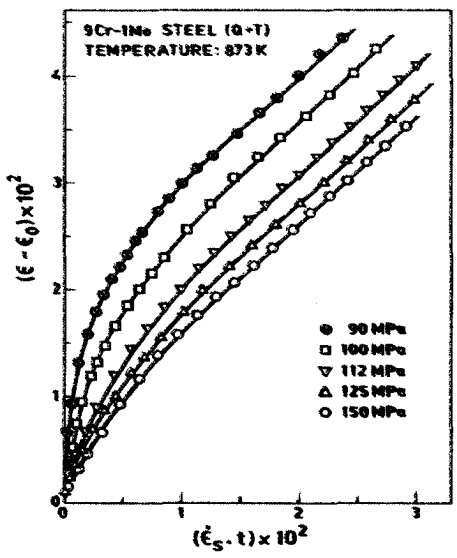

Fig. 6 $(\epsilon - \epsilon_0)$ vs $\dot{\epsilon}_s.t$ plots for 9Cr-1Mo steel at 873 K

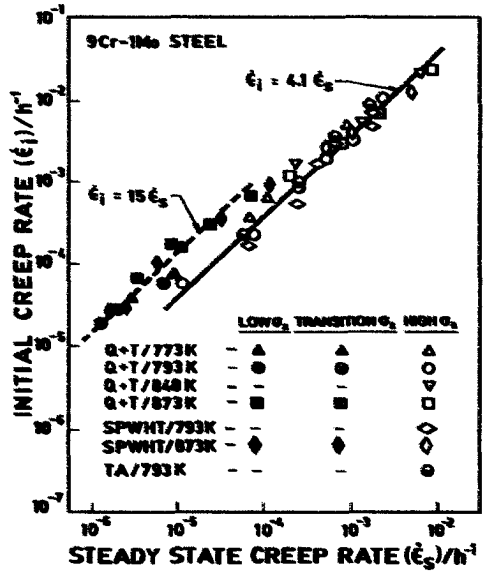

Fig. 8 Plot of $\dot{\epsilon}_i$ against $\dot{\epsilon}_s$ showing separate β values for low and high stress regimes

varied with stress and temperature. In this context, it is interesting to recall the relationship

$$(\dot{\epsilon}_s^{\alpha}.t_{os})/\epsilon_T = \text{constant}, \quad (5)$$

suggested by Phaniraj et al.[6] and for conditions obeying first order kinetics, i.e. $\alpha = 1$, Eq. (5) takes the form

$$(\dot{\epsilon}_s.t_{os})/\epsilon_T = \text{constant} = C_{PC}. \quad (6)$$

Further, for conditions obeying first order kinetics ($\alpha = 1$), they reformulated Eq. (3) in terms of a parameter $p' = \dot{\epsilon}_s.t/\epsilon_T \geq 0$ ($p' = 0$ at $t = 0$ and $p' = C_{PC}$ at t_{os}) as

$$\epsilon - \epsilon_0 = \epsilon_T [1 - \exp\{-p'(\beta - 1)\} + p']. \quad (7)$$

An important implication of Eq. (7) is that when ϵ_T varies and for conditions obeying first order kinetics, i.e. $\alpha = 1$, a plot of $(\epsilon - \epsilon_0)/\epsilon_T$ vs p' (i.e. $p' = \dot{\epsilon}_s.t/\epsilon_T$) would result in a master creep curve, only if β = constant. The results at all test conditions obeyed Eq. (6) with $\alpha = 1$ confirming the validity of first order kinetics. It is seen that irrespective of test temperature, the results yield separate master curves following Eq. (7), one for high stress regime (**Fig. 9**) and another for low stress regime (**Fig. 10**). Solid line in these figures corresponds to the theoretical curve according to Eq. (7) with β = 4.1 and 15 for high and low stress regimes, respectively. Both these master curves are shown in **Fig. 11**. The manifestation of two stress regimes with different values of stress exponent in terms of separate master creep curves with different values of β reflect the differences in the development of steady state structure from the initial structure, i.e. a high value of β = 15 at low stresses implies that the steady state and initial dislocation structures are farther apart. These observations further support the interpretation of steady state creep in terms of change in mechanism from climb by-pass over particles at low stresses to Orowan bowing at high stresses. The Orowan bowing operating at high stresses leaves dislocation loops and the rate of creep is determined by the rate at which the loop nearest to the particle climbs

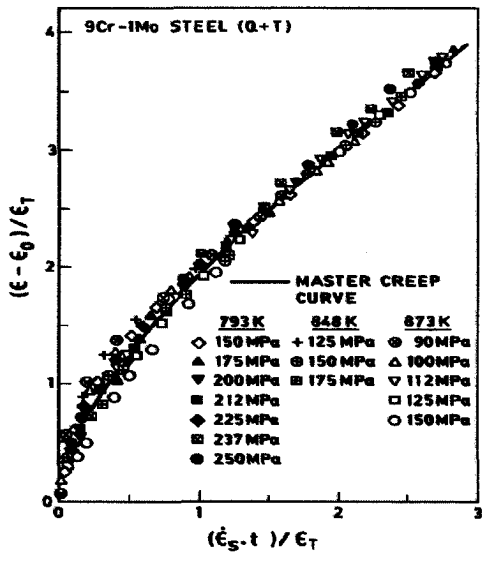

Fig. 9 Master creep curve according Eq. (7) for high stress regime at various temperatures

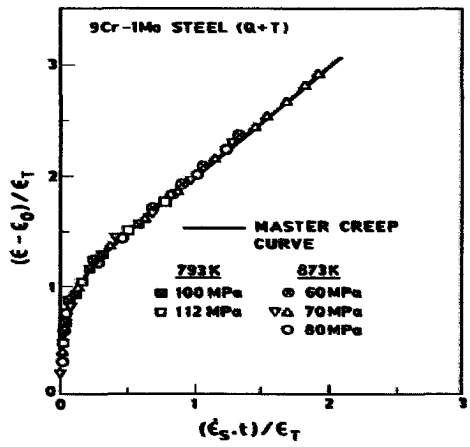

Fig. 10 Master creep curve according to Eq. (7) for low stress regime

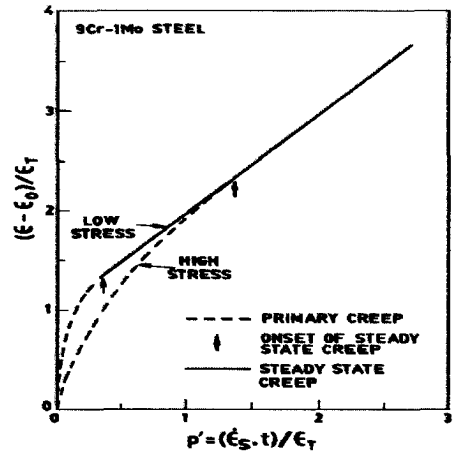

Fig. 11 Separate master creep curves for low and high stress regimes with β = 15 and 4.1 for the respective regimes

over and gets annihilated.[24] The analysis of transient creep reinforces that creep deformation in both the stress regimes is controlled by dislocation climb process.

3.2. Tertiary creep

The first order kinetic approach is extended to tertiary creep and for the analysis, we use the results obtained on 9Cr-1Mo steel at 793 and 873 K for Q + T and SPWHT conditions. Along similar lines to the concept of transient creep, it has been proposed[7,25] that the rate of increase in creep rate during tertiary creep could be predicted by assuming that the rate of change of creep rate is proportional to the difference between the tertiary and steady state creep rate values. It has been observed[7,25] that the tertiary creep obeyed first order kinetics with a rate constant p ($p = K'\dot{\epsilon}_s$) that depends on stress and temperature in the same way as does the steady state creep rate (i.e. K' is a constant). Recently, Phaniraj et al.[7] found that the strain-time data over the entire creep curve could be described by the relation

$$\epsilon = \epsilon_0 + \epsilon_T [1 - \exp(-r.t)] + \epsilon_t \exp[p(t - t_r)] + \dot{\epsilon}_s.t, \quad (8)$$

where ϵ_t is the limiting tertiary creep strain, t_r is the rupture life, and p is the rate of acceleration of tertiary creep and is the same as the rate constant when tertiary creep obeys first order kinetics. They also correlated the steady state and tertiary creep in terms of remnant strain ϵ_R (i.e. $\epsilon_R = \epsilon_f - \epsilon$; ϵ_f is the strain at fracture) and remnant time t_R (i.e. $t_R = t_r - t$) as

$$\epsilon_R = (\beta'-1)/K' \ [1-\exp(-K'\dot{\epsilon}_s.\ t_R)] + \dot{\epsilon}_s.t_R\ . \qquad (9)$$

where $(\beta' - 1)/K' = \epsilon_t$, β' is a constant and is the ratio of final creep rate $\dot{\epsilon}_f$ to $\dot{\epsilon}_s$. It may be emphasised that ϵ_t is a constant, since β' and K' are constants. Further for a constant ϵ_t, Eq. (9) yields a single master curve when the data is plotted as ϵ_R vs $\dot{\epsilon}_s.t_R$. ϵ_t was obtained from the creep curve as the intercept strain at $t = t_r$ and the procedure used for evaluating r was adopted for determining p by treating tertiary as a reverse of transient creep. The final creep rate $\dot{\epsilon}_f$ was calculated as $\dot{\epsilon}_f = \dot{\epsilon}_s + p\epsilon_t$ which follows from Eq. (8).

The creep data were adequately described by Eq. (8). Unlike r, the tertiary creep parameter p exhibited the same stress dependence as $\dot{\epsilon}_s$ in both the stress regimes. When steady state and tertiary creep obey first order kinetics, proportionality is observed between $\dot{\epsilon}_f$ and $\dot{\epsilon}_s$ (i.e. $\dot{\epsilon}_f = \beta'\dot{\epsilon}_s$) and between p and ϵ_s (i.e. $p = K'.\epsilon_s$); the validity of these relationships is shown in **Figs. 12** and **13**, respectively for the results at 873 K. It is interesting to note that the results in the two stress regimes yield a separate set of constant values of β' and K', i.e. $\beta' = 105$, $K' = 230$ and $\beta' = 48$, $K' = 110$ for low and high stress regimes, respectively. The high stress data at 793 K also obeyed these relationships. For 9Cr-1Mo steel, Eq. (9) could not provide the unified description in terms of master creep curve when ϵ_R is plotted against $\dot{\epsilon}_s.t_R$ because of scatter observed in the value of ϵ_t (e.g. $\epsilon_t = 41 \pm 5$ % for the results at 873 K). In this context, it is interesting to recall the relationship

$$(\dot{\epsilon}_s^{\alpha'}.t_t)/\epsilon_t = \text{constant}\ , \qquad (10)$$

suggested by Phaniraj et al.[7], where t_t is the time spent in tertiary creep. For conditions obeying first order kinetics, i.e. $\alpha' = 1$, Eq. (10) takes the form

$$(\dot{\epsilon}_s.t_t)/\epsilon_t = \text{constant} = C_{TC}\ . \qquad (11)$$

For conditions obeying first order kinetics ($\alpha' = 1$), they introduced a parameter $p'' = (\dot{\epsilon}_s.t_R)/\epsilon_t \geq 0$; $p'' = 0$ at $t_R = 0$ (i.e. at $t = t_r$) and $p'' = C_{TC}$ at $t_R = t_t$ (i.e. at $t = t_{ot}$, the time for the onset of tertiary creep). We reformulate Eq. (9) in terms of p'' as

$$\epsilon_R = \epsilon_t\ [1 - \exp\ \{-p''\ (\beta' - 1)\} + p'']\ . \qquad (12)$$

An important implication of Eq. (12) is that for conditions obeying first order kinetics (i.e. $\alpha' = 1$) and when ϵ_t varies or shows scatter as observed for 9Cr-1Mo steel, a plot of ϵ_R/ϵ_t vs p'' (i.e. $\dot{\epsilon}_s.t_R/\epsilon_t$) would result in a master creep curve only if β' = constant. The results at all test conditions obeyed Eq. (11) with $\alpha' = 1$ confirming the validity of first order kinetics. Our attempts to obtain master creep curve described by the new Eq. (12) resulted in separate master curves, one for high stress regime (**Fig. 14**) and another for low stress regime (**Fig. 15**) for the results at 873 K. Solid line in these figures corresponds to the theoretical curve according to Eq. (12) with $\beta' = 47$ and 100 (for Q + T condition) for high and low stress regimes, respectively. Both these master curves are shown in **Fig. 16**. It is important to recall that 9Cr-1Mo steel did not show any evidence of typical intergranular creep damage.[17] The focal point of the analysis presented so far is that in both the stress regimes, steady state and tertiary

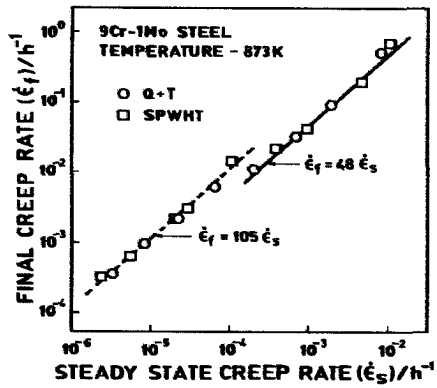

Fig. 12 Plot of $\dot{\epsilon}_f$ against $\dot{\epsilon}_s$ showing separate β' for low and high stress regimes at 873 K

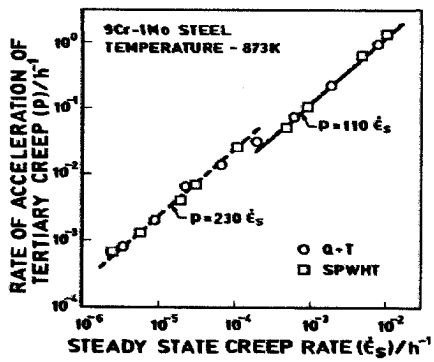

Fig. 13 Plot of p vs $\dot{\epsilon}_s$ illustrating separate K' for low and high stress regimes at 873 K

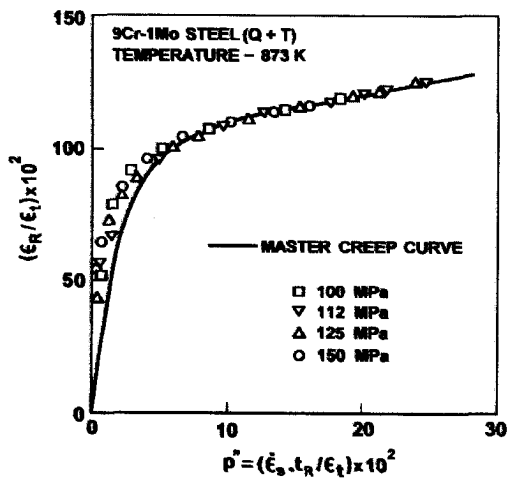

Fig. 14 Master creep curve according to Eq. (12) for high stress regime at 873 K

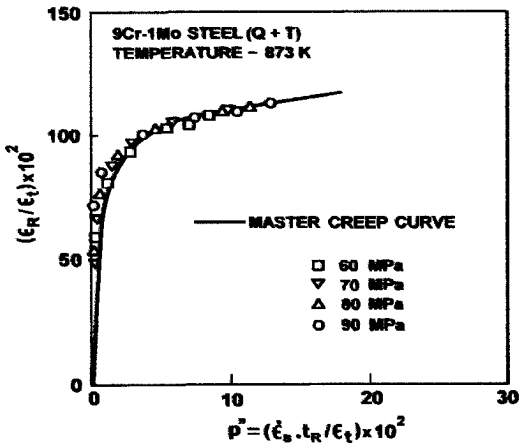

Fig. 15 Master creep curve according to Eq.(12) for low stress regime at 873 K

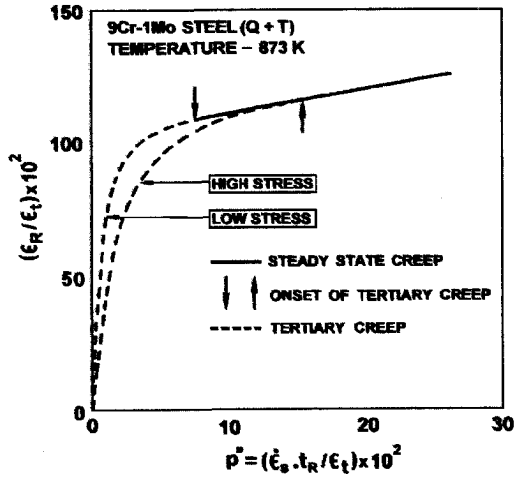

Fig. 16 Separate master creep curves for low and high stress regimes at 873 K with β' = 100 and 47 for the respective regimes

creep are related by a single master curve and tertiary creep is governed by first order kinetic process. This suggests that the mechanism of tertiary creep is not different from that operating in the steady state regime; the same dislocation climb controlled recovery process but with rate of recovery accelerating during tertiary creep. This is in accordance with the observation by Phaniraj et al.[7] and further lends support to the explanation put forward earlier[17] that the prolonged tertiary creep and high ductility observed in 9Cr-1Mo steel is attributed to the increased extent of recovery associated with coarsening of precipitates and subgrains.

3.3. Interesting relationships

The useful implications of the relationships proposed for transient and tertiary creep [i.e. Eqs. (5) and (10)] in understanding Monkman-Grant (MGR: $\dot{\epsilon}_s^m.t_r$ = constant) and modified Monkman-Grant (MMGR: $\dot{\epsilon}_s^{m'}.t_r/\epsilon_f$ = constant) relationships are presented in the following. The validity of Eqs. (5) and (10) along with MGR and MMGR for the results at 873 K is illustrated typically in **Figs. 17** and **18**, respectively; the values of α, α', m and m' are

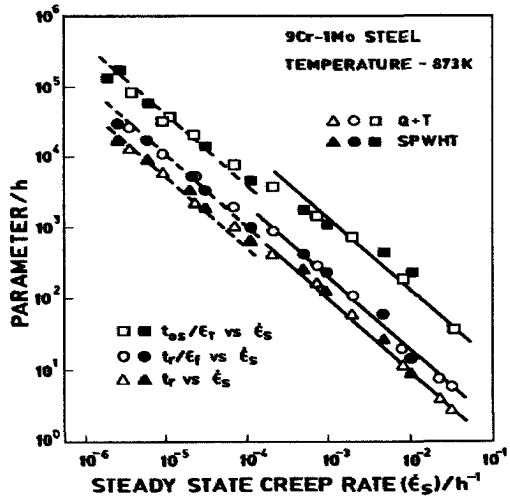

Fig. 17 Analogy of Eq. (6) with MGR and MMGR for tests at 873 K illustrating separate values of C_{PC} = 0.35 and 1.35 for low and high stress regimes respectively

found to be close to unity. From the values of α and α' = 1, we show the validity of Eqs. (6) and (11), and the first order kinetics for 9Cr-1Mo steel. These results are in agreement with those reported by Phaniraj et al.[6,7] But the interesting observation to note here is that the two stress regimes with different stress exponents are manifested as separate set of constant values of transient and tertiary creep constants (C_{PC} and C_{TC}) along with Monkman-Grant ($C_{MG} = \dot{\epsilon}_s.t_r$) and modified Monkman-Grant ($C_{MMG} = \dot{\epsilon}_s.t_r/\epsilon_f$) constants. The distinct values of C_{PC} and C_{TC} observed in the two stress regimes are also reflected in **Figs. 11** and **16**, respectively as separate master curves for the respective stress regimes. It is worthwhile to recall[17] that the two stress regimes were manifested in terms of different values of creep damage tolerance factor λ ($\lambda = 1/C_{MMG}$) for 9Cr-1Mo steel. Along similar lines, we examine the creep data obtained by Ennis et al.[5,26] for a P92 (NF616) steel (temperature range 873-948 K, stress range 82-180 MPa) to understand the

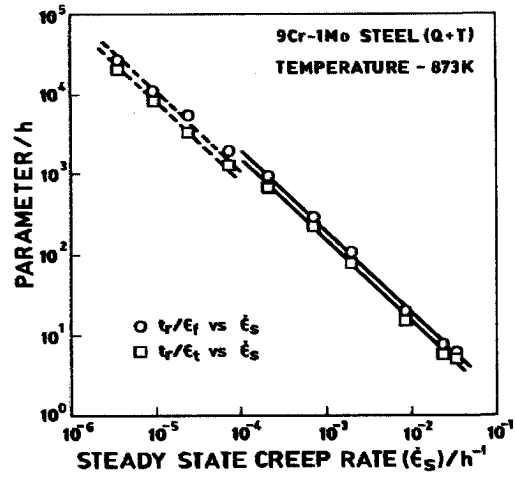

Fig.18 Analogy of Eq. (11) with MMGR for tests at 873 K illustrating separate values of C_{TC} = 0.08 and 0.16 for low and high stress regimes respectively

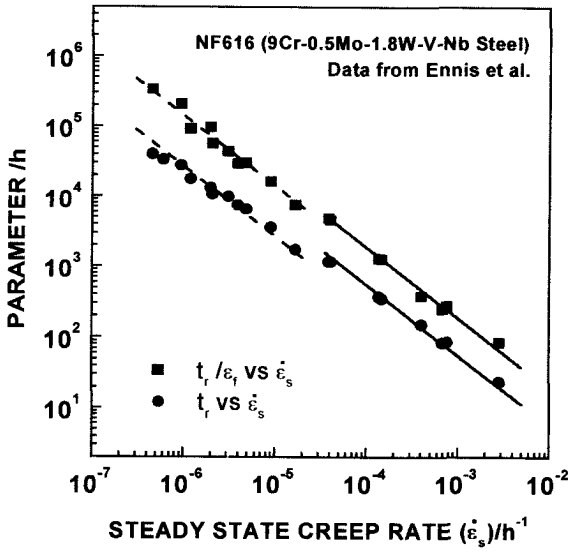

Fig 19 Plot of MGR and MMGR for P92 steel showing separate values of C_{MG} and C_{MMG} in the respective stress regimes

reported different stress regimes[5] in terms of creep rate-rupture life relationships and damage tolerance factor. A close analysis of their data revealed that the two stress regimes are characterized by a separate set of constant values of λ and ϵ_f ; $\lambda \sim 7$, $\epsilon_f = 20$ % at low stresses and $\lambda \sim 5$, $\epsilon_f = 30$ % at high stresses. This prompted us to classify the stress regimes in terms of separate constant values of C_{MG} and C_{MMG}, and is shown in **Fig. 19** for the P92 steel. These observations are in accordance with the results presented for 9Cr-1Mo steel and further imply that the first order kinetic approach can be extended to advanced 9Cr-1Mo steels.

4. Concluding Remarks

The deviations in the stress exponent and apparent activation energy observed for 9Cr-1Mo steel are rationalized by invoking the concept of resisting stress and led to meaningful conclusion that creep is governed by dislocation climb process in both the stress regimes. The analysis of first order kinetics for transient and tertiary creep further exhibited different manifestations like separate master creep curves in the respective stress regimes. The synthesis of creep behaviour in terms of relationships proposed for transient and tertiary creep not only provides proper interpretation of existing creep rate-rupture life relationships of Monkman-Grant type, but might also bear implications for realistic extrapolation of rupture lives. We advocate the importance of detailed analysis of different stages of creep as described in this paper for meaningful interpretation of totality of creep deformation and fracture.

Acknowledgements – The authors thank Mr P.J.Ennis, Research Centre Juelich, Germany for providing creep data of P92 steel. The authors also thank Dr. Placid Rodriguez and Dr. Baldev Raj, Indira Gandhi Centre for Atomic Research, Kalpakkam for their constant encouragement.

REFERENCES

1) D. A. Miller: *Mater. Sci. Eng.*, **54** (1982),169.
2) R. Singh and S. Banerjee: *Acta Metall. Mater.*, **40** (1992), 2607.
3) R. S. Fiddler: *CEGB Report - RD/L/R* 1949 (1976).
4) B. J. Cane and R. S. Fiddler: Ferritic Steels for Fast Reactor Steam Generators, British Nuclear Energy Society, London (1977), 193.
5) P. J. Ennis, A. Zielinska-Lipiec, O. Wachter and A. Czyrska-Filemonowicz: *Acta Mater.*, **45** (1997), 4901.
6) C. Phaniraj, M. Nandagopal, S. L.Mannan, and P. Rodriguez: *Acta Metall Mater.*, **39** (1991), 1651.
7) C. Phaniraj, M. Nandagopal, S. L. Mannan, P. Rodriguez and B. P. Kashyap: *Acta Mater.*, **44** (1996), 4059.
8) B. K. Choudhary C. Phaniraj, K. Bhanu Sankara Rao and S. L. Mannan: Proc. 8th Int. Conf. Creep and Fracture of Engineering Materials and Structures, Tsukuba, Japan (1999), (eds) T. Sakuma, and K. Yagi, *Key Eng. Materials*, **171-174** (2000), 437.
9) B. K. Choudhary C. Phaniraj, K. Bhanu Sankara Rao and S. L. Mannan: Proc. Int. Symp. Materials Ageing and Life Management, ISOMALM 2000, Kalpakkam (2000), 675.
10) F.C. Monkman and N.J. Grant: *Proc. Am. Soc. Test. Mater.* **56** (1956), 593.
11) F. Dobes and K. Milicka: *Metal Sci.*, **10** (1976), 382.
12) A. K. Mukherjee, J. E. Bird and J. E. Dorn: *ASM Trans. Quart.*, **52** (1969), 155.
13) R. Lagneborg and B. Bergman: *Metal Sci.*, **10** (1976), 20.
14) M. Mc Lean: *Acta Metall.*, **33** (1985), 545.
15) B. K. Choudhary: Ph. D. Thesis, Indian Institute of Technology, Bombay (1997).
16) B. K. Choudhary, K. Bhanu Sankara Rao and S. L. Mannan: *Trans. Indian. Inst. Metals*, **52** (1999), 327.
17) B. K. Choudhary, S. Saroja, K. Bhanu Sankara Rao and S. L. Mannan: *Metall. Mater. Trans.*, **30A** (1999), 2825.
18) H. J. Frost and M. F. Ashby: Deformation Mechanism Maps - The plastic and Creep of Metals and Ceramics, Pergamon Press, (1982).
19) C. Phaniraj: Ph. D. Thesis, Indian Institute of Technology, Bombay (1997).
20) G.A. Webster, A.P.D. Cox and J.E. Dorn: *Metal Sci. J.*, **3** (1969), 221.
21) K.E. Amin, A.K. Mukherjee and J.E. Dorn: *J. Mech. Phys. Solids*, **18** (1970), 413.
22) A. Ahmadieh and A.K. Mukherjee: *Mater. Sci. Eng.*, **21** (1975), 115.
23) F. Garofalo: Fundamentals of Creep and Creep Rupture in Metals, Mc Millan, New York (1965).
24) G. S. Ansel and J. Weertman: *Trans. Metall. Soc. AIME.*, **215** (1959), 838.
25) W. J. Evans and B. Wilshire, *Metall Trans.*, **1** (1970), 2133.
26) P. J. Ennis, KFA Juelich, Germany-Private Communication.